Conspicuous phases between P and S arrivals observed in the DPRI seismic network

AUTHOR(S):

NAKAMURA, Mamoru; ANDO, Masataka

CITATION:

NAKAMURA, Mamoru ...[et al]. Conspicuous phases between P and S arrivals observed in the DPRI seismic network. Bulletin of the Disaster Prevention Research Institute 1995, 45(1): 1-16

ISSUE DATE:

1995-03

URL:

http://hdl.handle.net/2433/125007

Bull. Disas. Prev. Res. Inst., Kyoto Univ., Vol. 45, Part 1, No. 387, March, 1995

Conspicuous phases between P and S arrivals observed in the DPRI seismic network

By Mamoru NAKAMURA and Masataka ANDO

(Manuscript received on August 4, 1994. revised on December 8, 1994)

Abstract

In central Honshu, Japan, numerous phases between P and S arrivals are frequently observed in seismograms of deep earthquake events. We show in this paper some examples of seismograms of these later phases. From the seismograms in the events of the Hokkaido and Ryukyu regions, we can observe triplication resulting from seismic discontinuity at depths of 410 km and 660 km. Some of later phases observed at events occurring below the Japan Sea region may be related to an anomalous low velocity structure in the upper mantle beneath eastmost Asia. Moreover, we observe some later phases which are generated at the upper portion of the slab or within the slab interface. Using travel time of observed later phases, we estimate that layer structure exists within slab at the depth of 100–150 km and deep earthquakes occur 20 km apart from upper slab interface at the depth of 300–500 km. Moreover, another later phase is observed in the deep events of the Bonin region. Apparent velocity of the later phase is much smaller than that of direct P, which implicates that the later phase is trapped in the crust or uppermost mantle beneath the Nankai trough. We can not, however, explain the nature of all the observed later phases in the present paper.

1. Introduction

Later phases of direct P have so far been reported in Japanese seismological stations. In previous studies, PS and SP phases which were converted from P to S or S to P at the upper slab interface were used to determine the location of upper slab interface in the Tohoku region (Matsuzawa et al., 1986; Matsuzawa et al., 1990). In the Kanto region, the upper slab interface was determined using SS phase which is reflected from the upper slab interface (Obara, 1989). Near the western Chubu area, later phases were recorded from events on the Philippine Sea (PHS) plate (Hori et al., 1985). Hori et al. (1985) showed that a low velocity zone exists on the PHS plate and inferred the presence of an oceanic crust subducting down to a depth of 60 km below the western Chubu area. Using these phases, they also confirmed the configuration of the slab structure of the Pacific and PHS plates.

Studies of later phases are thus useful in understanding the nature of the subducting slab and the interface between the slab and the surrounding mantle. Such studies are also useful in determining the velocity contrast at the upper mantle interface.

The central Japan region overlies the Philippine Sea (PHS) plate and the Pacific plate where many deep earthquakes occur. We observed anomalous phases appearing on short-period seismograms of the Disaster Prevention Research Institute (DPRI) seismological net-

work of Kyoto University. Many of the observed phases are generated in the crust or near the stations but some phases are certainly derived from reflectors near the hypocenters. Triplication at 410 km and 660 km discontinuity also contributes to the generation of the observed later phases while some phases are possibly related to scatterers near the slab. We can show the origin of some later phases. However, the cause of other phases has not been made clear. In this paper, we show examples of the later phases.

2. Station and data

The DPRI seismological network, located in central Japan, spans 200 km by 300 km and consists of 30 stations. The network is collectively called SWARMS (Seismic Wave Automatic Recording and Measuring System) (Disaster Prevention Research Institute, Kyoto University, 1986). Wide coverage of the network thus makes it ideal to accurately measure apparent velocity, which is useful to understand the origin of later phases. Events used in this study are located in the Izu-Bonin, Japan Sea, and the Hokkaido regions. The events have depths of more than 100 km and magnitudes greater than 3.3. We use the vertical components of short-period seismograms recorded in the DPRI network from 1985–1993 (**Fig. 1, Table 1**) with the sampling frequency set at 100 Hz. In the following text, we show examples of seismograms of the observed anomalous later phases, and classify these phases, for each of the

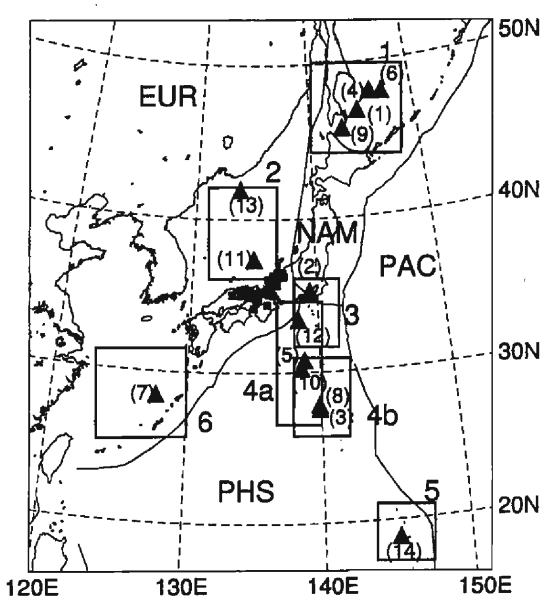

Fig. 1. Distribution of seismic stations and earthquake epicenters. Solid rectangles show stations of the DPRI seismological network and triangles show epicenters of deep earthquakes used in this study. Open rectangles 1 to 6 show the regions classified in this study. 1=Hokkaido region; 2=Japan Sea region; 3=Izu-Bonin region (intermediate depths); 4a, b= Izu-Bonin region (deep events); 5=Mariana region; 6=Ryukyu region. EUR=Eurasian plate; PAC=Pacific plate; NAM=North American plate; PHS=Philippine Sea plate.

Table 1. List of deep earthquakes used in this study

Event	*Origin*		*Latitude*	*Longitude*	*Depth*	*Magnitude*
	Date	*Time, UT*	°N	°E	km	mb
1	Jul. 05, 85	2 : 38 : 17.6	46.84	144.62	370	5.1
2	Aug. 08, 85	5 : 35 : 24.3	35.31	139.40	123	4.4
3	May 17, 86	13 : 19 : 00.4	27.56	139.89	489	4.6
4	Jun. 02, 86	19 : 29 : 56.5	48.04	145.98	461	5.1
5	Dec. 14, 86	8 : 39 : 29.7	30.79	138.81	422	4.5
6	Apl. 14, 87	13 : 12 : 19.5	47.95	147.12	421	4.5
7	May 03, 87	17 : 21 : 22.6	28.45	127.69	209	5.1
8	Jan. 22, 89	17 : 29 : 45.5	27.83	139.86	528	4.6
9	Feb. 04, 89	6 : 52 : 54.7	45.75	143.04	315	4.8
10	Aug. 05, 89	5 : 41 : 52.6	30.25	138.57	436	4.4
11	Sep. 15,89	2 : 37 : 06.7	37.40	134.96	388	3.3
12	May 23, 90	17 : 47 : 30.5	33.47	138.43	308	4.3
13	Nov. 24, 90	17 : 24 : 37.9	41.92	133.69	455	4.8
14	Jul. 30, 91	9 : 39 : 40.0	18.88	145.16	599	4.9

following areas (**Fig. 1**) :

1. Hokkaido region
2. Japan Sea region
3. Izu-Bonin region (intermediate depths)
4. Izu-Bonin region (deep events)
5. Mariana region
6. Ryukyu region

3. Seismograms of later phase

3. 1 Hokkaido region

In the Hokkaido region, deep seismicity is high. For this region, anomalous arrivals are observed for events deeper than 300 km. These events are distributed at depths of 300–500 km and are located north of Hokkaido and around the Okhotsk area. The waveforms of these events show apparent double phases (**Fig. 2a-d**). These phases are observed in almost all stations of the DPRI network except for deep earthquakes west of Tohoku and west of the Japan Sea region.

The X–P time delays for event 9 (Fig. 2a) are 3.7 s and 1.9 s, at epicentral distances of 1130 km and 1400 km, respectively. For this event, apparent velocities of P and X phases are 9.5 km/s and 10.5 km/s, respectively. For event 1 (Fig. 2d), however, apparent velocities of the P and X phases are 10.5 km/s and 9.5 km/s, respectively. In the first case, the amplitude of the X phase is the same as that of P phase (**Fig. 2a-c**) while in the latter case, the amplitude of X phase is larger than that of P phase (**Fig. 2d**). Based on the epicentral distance and hypocentral depth, we interpret these phases as branches of triplication at the 410 km and 660 km discontinuities.

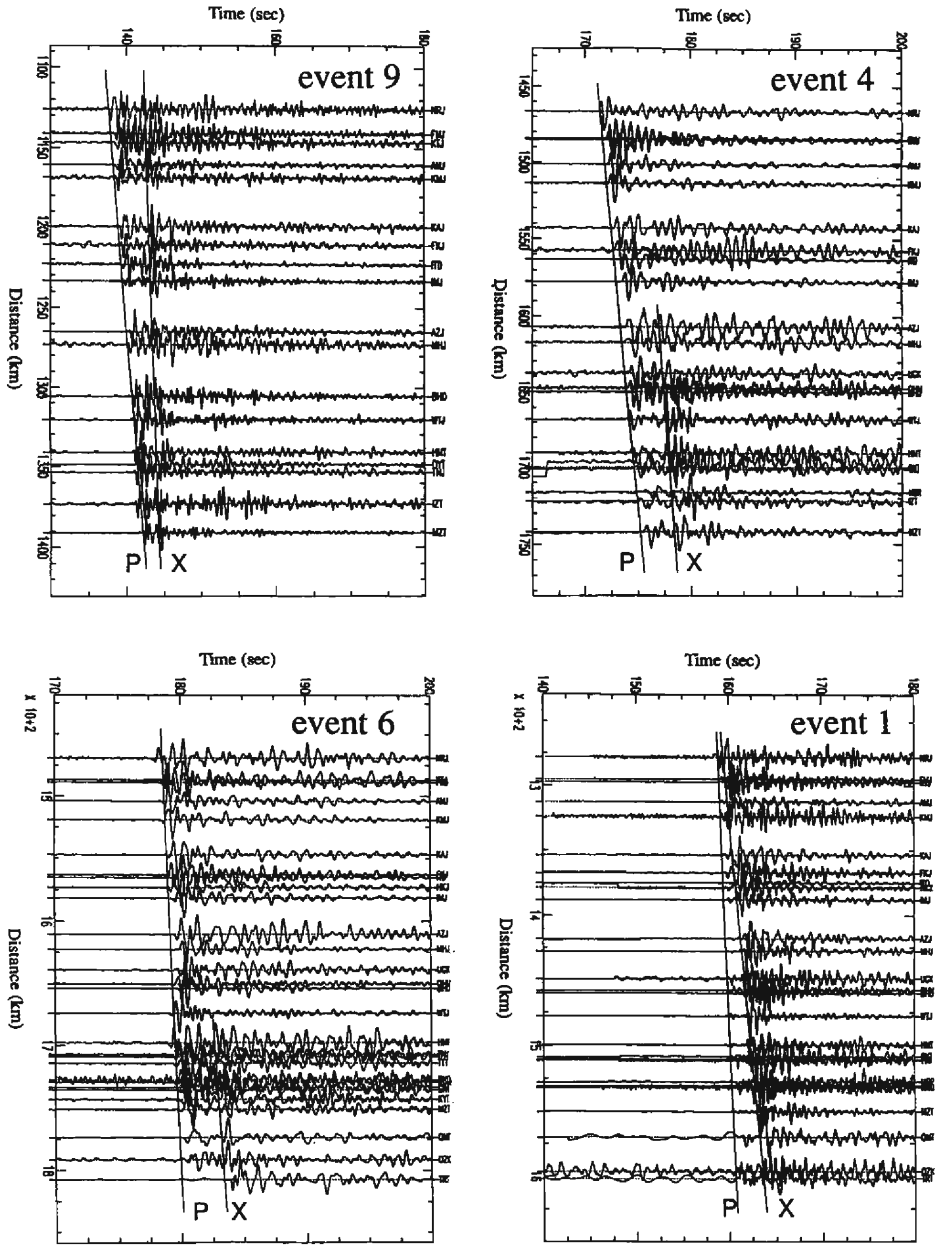

Fig. 2. Observed seismograms of a later phase from earthquakes which occurred at the Hokkaido region. The time scale is reduced to t-D/Vr where D and Vr is the epicentral distance and reduced velocity, respectively. Initial and later arrivals are indicated by solid lines. Seismograms are filtered to pass the frequency bands of 0.5–2.0 Hz. (a); Event 9. Reduced velocity is 10.5 km/s. (b); Event 4. Reduced velocity is 13.0 km/s. (c); Event 6. Reduced velocity is 11.5 km/s. (d); Event 1. Reduced velocity is 11.0 km/s.

3. 2 Japan Sea region

Seismicity is lower in this area than that in the Hokkaido and the Izu-Mariana regions. North of the Japan Sea region, a deep earthquake occurred at a depth of 455 km which is followed by many later phases within 20–30 s after the P arrivals (**Fig. 3**). A conspicuous phase can be observed occurring 10–13 s after the P arrival. Apparent velocity of this phase is 9.6 km/s, which is smaller than that of P phase (10.2 km/s). The amplitudes of these phases are smaller than or the same as those of the P phases. The apparent velocity of some later phases is smaller than that of the P phase, which indicates that these phases may be generated above the slab. Since the apparent velocity of the later phase is larger than P-wave velocity at the crust, the later phases are possibly generated at wedge mantle above the slab. A similar phase is not observed for events in the Izu-Mariana region while anomalous later phases are more commonly observed for the events in this area compared with deep events in other regions, which suggests that there is a very reflective interface around the slab that forms part of a complicated structure below Japan Sea.

In addition, deep seismicity is very high to the north off the Kinki district. Later phases are observed 2–3 s after the P arrivals for some of these events (**Fig. 4**). Since these phases are also observed in the Izu-Bonin region, we defer discussion of these phases to section 3. 4. (1).

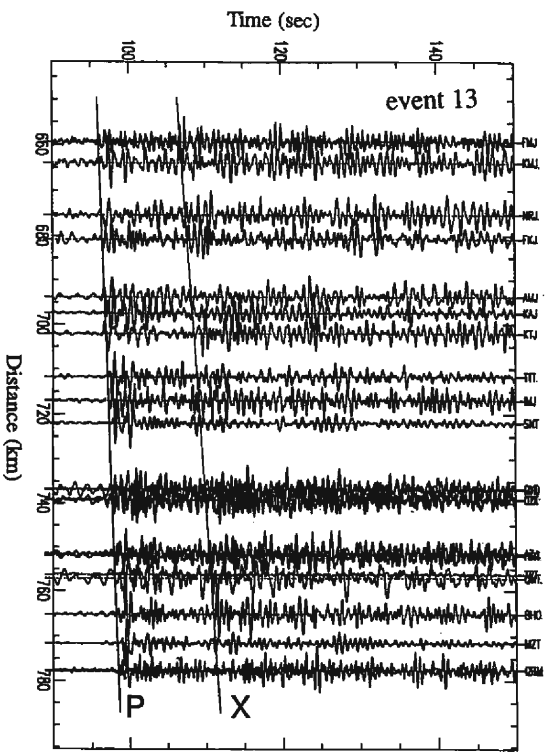

Fig. 3. Seismogram of event 13 which occurred north of the Japan Sea region. Time scale is reduced to t-D/13.0 (km/s). Initial and later arrivals are indicated by solid lines. Seismograms are filtered to pass the frequency bands of 0.5–2.0 Hz.

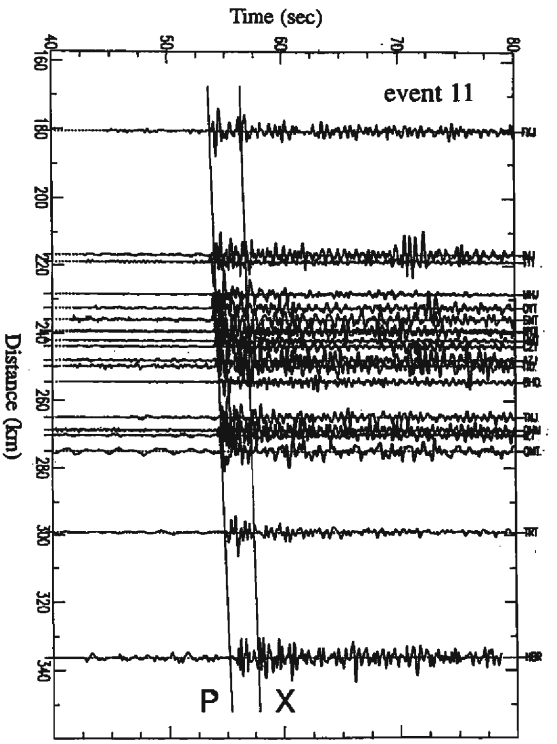

Fig. 4. Seismogram of event 11 which occurred south of the Japan Sea region. Time scale is reduced to t-D/20.0 (km/s). Initial and later arrivals are indicated by solid lines. Seismograms are filtered to pass the frequency bands of 0.5–2.0 Hz.

3.3 Intermediate depth events at Izu-Bonin region

Depths of seismic events in the Izu-Bonin area vary from 60 to 200 km. **Fig. 5** is a seismogram of an intermediate-depth event which occurred in the area with the later phase arriving 9–11 s after the initial P phase. The later phase is not usually observed in most events. Event 2, which occurred at Kanagawa Prefecture, west of Kanto district, has an apparent later phase velocity of 10.0 km/s, which is greater than that of the P phase (8.6 km/s) (**Fig. 5**). The amplitude of the later phase is smaller than or the same as that of the P phase. From apparent velocity and X–P time delays, Ohkura et al. (1990) interpreted this phase as S converted and reflected to P within the slab. This interface is 30 km apart from the upper slab interface, which implies that a velocity discontinuity exists within the slab.

Analysis of velocity structure by Suyehiro and Sacks (1979) pointed out the existence of a double-layered structure in a descending slab. In the Kanto region, double P arrivals were noted and were characterized by a low frequency first arrival followed by a high frequency second arrival (Iidaka and Mizoue, 1991). The second phase was 1–3 s after the first arrivals. They argue that the second arrival is a reflection from an interface within the subducted slab. Their best fitting model includes a 30 km thick channel, 1.5% faster than J–B. Petrologically, the oceanic plate consists of two distinct peridotites (Ringwood and Irifune, 1988). However, it seems unlikely that a small difference between individual peridotites will produce such a

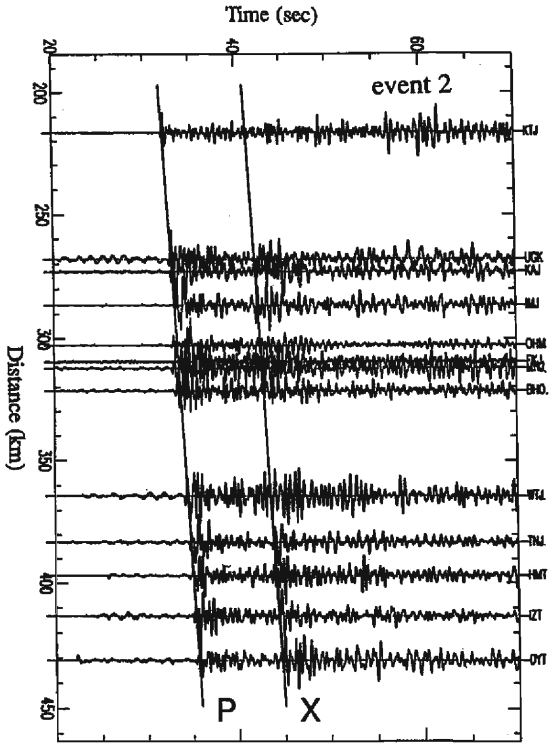

Fig. 5. Seismograms of event 2. Observed later phase is converted within the slab. Time scale is reduced to t-D/10.0 (km/s). Initial and later arrivals are indicated by solid lines. Seismograms are filtered to pass the frequency bands of 0.5–2.0 Hz.

marked velocity contrast (Helfrich et al., 1989). It is difficult to explain the origin of this interface.

Moreover, intermediate-depth earthquakes occur at this discontinuity. A double seismic zone has developed in the Tohoku and Kanto districts (Hasegawa et al, 1978 ; Ishida, 1984). Lower intermediate-depth earthquakes occur 30 km apart from the upper slab interface with the lower seismicity being located at the reflector earlier pointed out by Iidaka and Mizoue (1991). Intermediate-depth earthquakes occur at the discontinuity of seismic velocity, which implies that the boundary formation is related to the origin of the intermediate-depth earthquakes.

3. 4 Deep events at the Izu-Bonin region

In this area, we find two types of later phases distinguished on the basis of the difference of the apparent velocity between P and the later phase. These types are as follows :

Type (1) : Apparent velocity of the later phase is the same as that of the P phase.

Type (2) : Apparent velocity of the later phase is smaller than that of the P phase.

(1) SP phase converted at the slab interface

Later phases of events for the Izu-Bonin region arrive 2–3 s and 11–15 s after the P

arrivals. The X–P time delays are nearly constant for each event (**Fig. 6, 7a, b**). These phases have the same apparent velocity as the P phase. The amplitudes of the later phases are the same as or smaller than that of the P phase. Because X–P time delays would be 4–5 s if these phases are converted P-to-S at Moho, this idea could be excluded. To explain the apparent velocity and X–P time delays, S–P conversion near the slab is plausible ; first, the later phase is converted at the upper slab interface and then the second phase is reflected near the lower slab interface. Using the X–P time delays, the upper slab interface was located 20 km above the hypocenter and the lower interface was located 50–80 km below the hypocenter. These results indicate that deep earthquakes occur in the slab 20 km away from the upper slab interface. These data are also consistent with the results of high-pressure experiments where phase transformation of metastable olivine generates anti-crack faulting (Green and Burnley, 1989). This transformation occurs within a narrow temperature range. The contour of the temperature is parallel to the upper slab interface (Helfrich et al., 1989), which implies that if deep earthquakes occur at a narrow temperature range, the distribution of deep earthquakes must also be parallel to the slab interface. Hence, transformation of metastable olivine generates deep earthquakes (Wu et al., 1993).

Moreover, we interpret the second later phase as a reflected phase near the lower slab interface. We used a velocity model with J–B in the surrounding mantle and J–B plus 5 % in

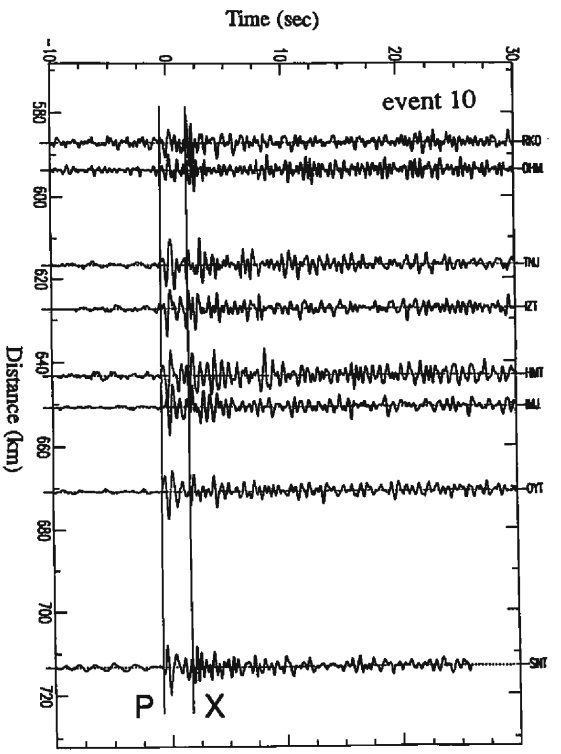

Fig. 6. Example of S-to-P converted phases at the upper slab interface for event 10. Time scale is reduced to t-D/14.0 (km/s). Initial and later arrivals are indicated by solid lines. Seismograms are filtered to pass the frequency bands of 0.5–2.0 Hz.

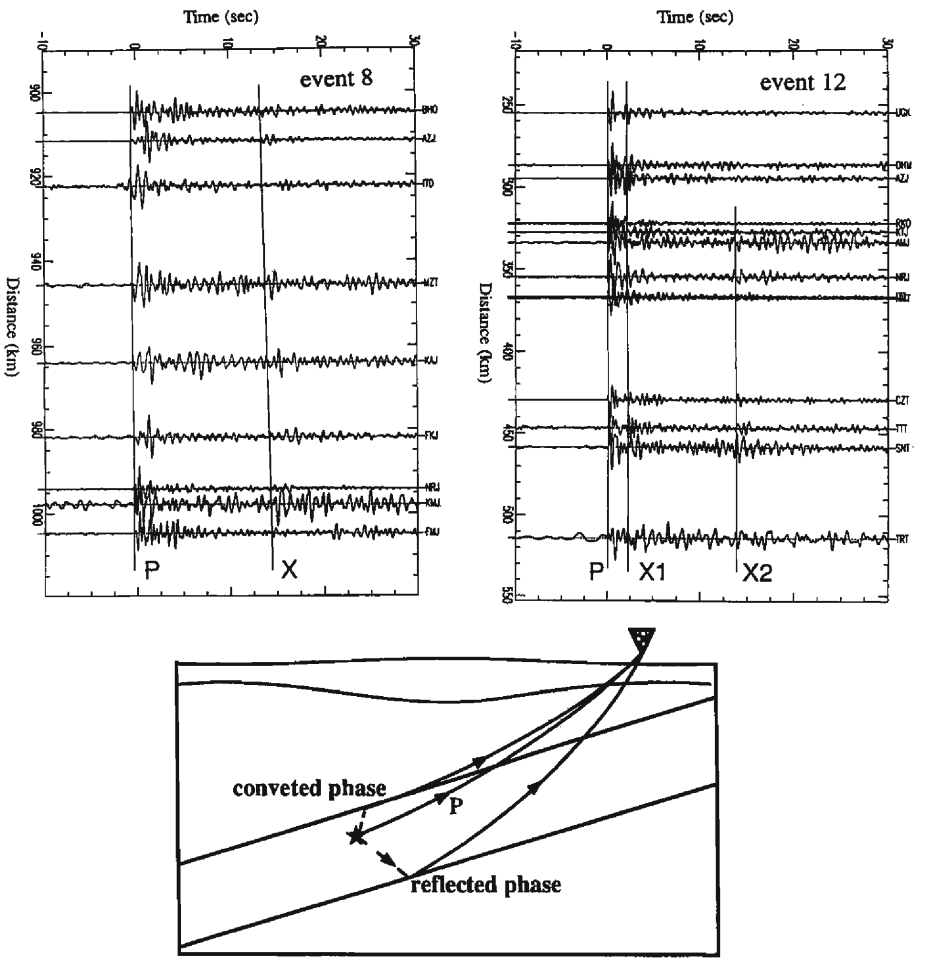

Fig. 7. (a) ; Seismogram of event 8. S-to-P converted phase near the lower slab interface was observed. Time scale is reduced to t-D/14.0 (km/s). (b) ; Seismograms of event 12. SP converted phases at the upper and lower slab interface are observed, denoted as X1 and X2, respectively. Initial and later arrivals are indicated by solid lines. Seismograms are filtered to pass the frequency bands of 0.5–2.0 Hz. (c) ; Schematic view of ray paths to the station for P, converted phase at the upper slab interface, and reflected phase near the lower slab interface.

the slab. However, the observed amplitude of the X2 phase is larger than the calculated one. A plausible model to account for this discrepancy is the focusing effect caused by undulation of reflector. At present, however, we do not have a plausible idea about the cause of the reflector near the lower slab interface. While we do not here discuss the origin of the later phase critically, we intend to discuss it precisely in another paper.

(2) Trapped phase at crust

Anomalous arrivals are confined to events north of about 27–30°N. The apparent

velocity of this phase is 7.1 km/s in event 3, which is smaller than that of the P phase (12.5 km/s) (**Fig. 8a**). In event 5 which occurred at 30°N (**Fig. 8b**), the amplitude of the later phase is the same as that of the P phase. This phase is observed in many stations (**Fig. 9a, b**). The apparent velocity of the later phases is the same as the P-wave velocity in the crust, which

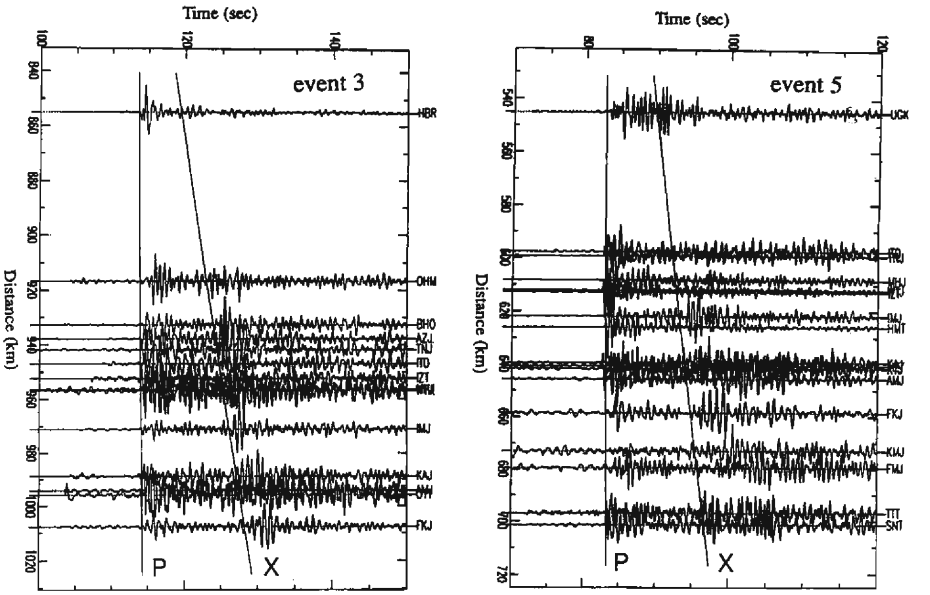

Fig. 8. (a) Seismogram of event 3. Reduced velocity is 12.5 km/s. (b) Seismograms of event 5. Reduced velocity is 12.0 km/s. Initial and later arrivals are indicated by solid lines. Seismograms are filtered to pass the frequency bands of 0.5–2.0 Hz.

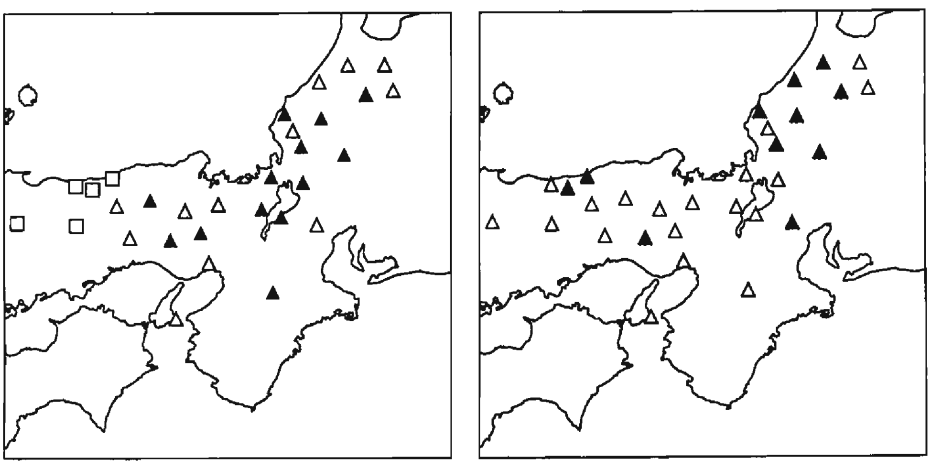

Fig. 9. (a) Distribution of stations where the later phase was observed in event 3. Solid and open triangles show stations where the later phase was observed and not observed, respectively. Rectangles show stations not triggered by this event. (b) Distribution of stations in the case of event 5.

shows that this phase passes horizontally through the crust. Moreover, in the case of event 3, the arrival of the X phase terminates with that of the P phase at the epicentral distance of 750 km, implying that the X phase originates at the epicentral distance of 750 km. Since the epicenter of event 3 is 27.5°N and 139.9°E, the X phase is generated at 33–34°N and 136–138°E (**Fig. 10a**). In the case of event 5, the epicentral distance at which P and X phases arrived at the same time is 370 km. The conversion point is again located at 33–34°N and 136–138°E. If the X phase is trapped at the midway between the hypocenter and station, we infer that the X phase is trapped at 33–34°N where the PHS plate subducts northwestward. Lateral heterogeneity is possibly greater than in other subduction areas so that trapped phases may result (**Fig. 10b**).

A similar phase was reported by Sekiguchi (1988) in the Hida region stations. Used events were located at the northwest of Japan Sea and depths of hypocenters were deeper than 500 km. The later phase was observed 11–14 s after the P arrival. In this case, the later phase was interpreted as a phase which was trapped between the junction of the island arc and the oceanic plate and eventually passed through the crust.

In the case of the Izu-Bonin region, the depth of Moho varies in the Nankai trough area because the crust changes from oceanic to island arc structure with a condition similar to that of the Japan Sea area. In our ray tracing calculations, however, the dip of the Moho discontinuity must be much greater than the actual dip in order to trap the direct P phase, which is impossible. Probably, the X phase may be a multi-reflected channel wave because the apparent velocity of the X phase is much smaller than that of the P phase.

A low velocity zone beneath the Nankai trough may produce trapped phases. In a previous study by Senna et al. (1990), their analysis of surface waves showed that a low velocity zone exists beneath the northern part of the PHS plate. Shear wave velocity at depths

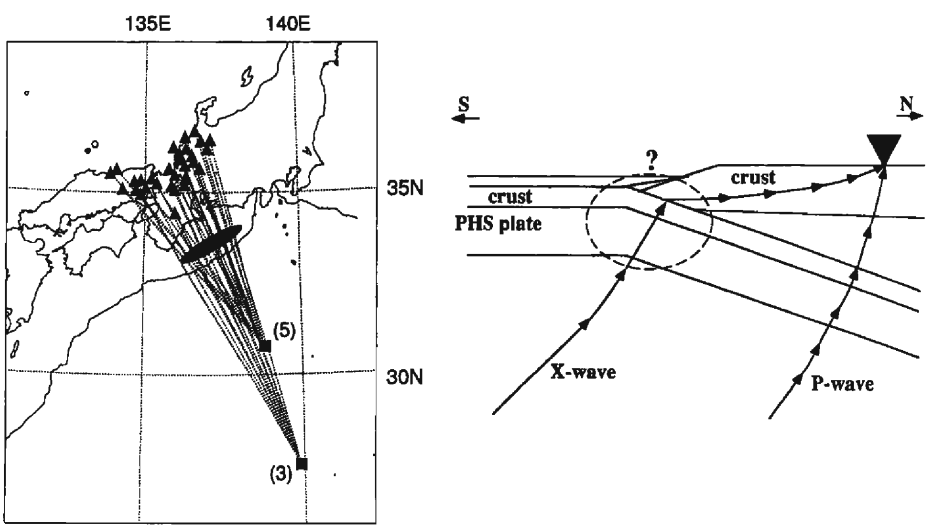

Fig. 10. (a) Great path circles (dashed lines) from hypocenter of events 3 and 5 to stations. Dashed ellipse shows the converted point. (b) Schematic representation of the ray paths of the P and X phases.

of 50–100 km is 4.2 km/s, which is 8.6% smaller than that of the overlying lithosphere. North of the Nankai trough region, moreover, there are thick sediments. The thickness of this sediment is 2–3 km (Park et al., 1990). Thus, a lateral low velocity zone of the uppermost mantle or thick sediments may generate the proposed trapped phases.

3. 5 A deep earthquake in the Mariana region

Later phases are also observed for event 14 which occurred in the Mariana region after the P phase (**Fig. 11**). These stations formed an elongated narrow zone trending northeast to southwest (**Fig. 12**). The source mechanism may affect the amplitude ratio between the direct P phase and the later phases. Apparent velocities of the two later phases are 15 km/s. The apparent velocity of the direct P phase is 14.0 km/s. One possible explanation for the first later phase is a branch of triplication at the 660 km discontinuity. However, the time delay between the P phase and the second later phase is 13 s, which is too late to explain in terms of a branch of triplication. An alternative explanation could be that this later phase was either a converted or reflected phase in the slab interface. We can not show the structure that would fit the arrival time of the second later phase because there are few events by which the second later phase could be observed. Hence, we can not fully explain the origin of the second later phase.

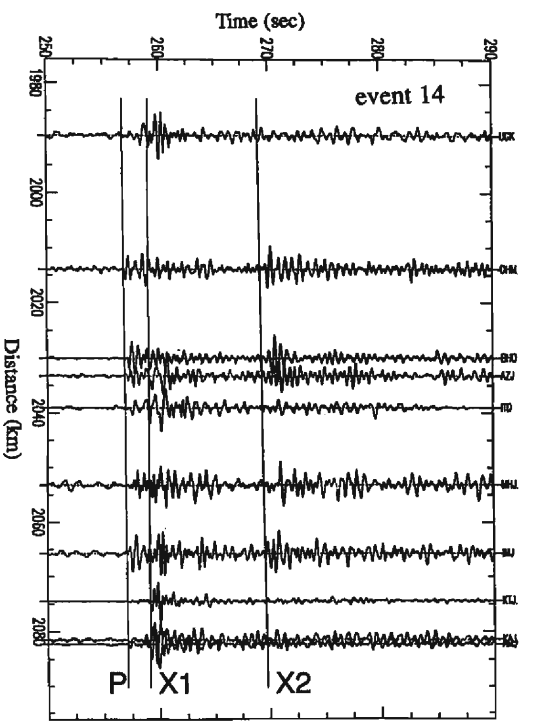

Fig. 11. Seismograms of event 14 which occurred in the Mariana region. Time scale is reduced to t-D/14.0 (km/s). Initial and later arrivals are indicated by solid lines. Seismograms are filtered to pass the frequency bands of 0.5–2.0 Hz.

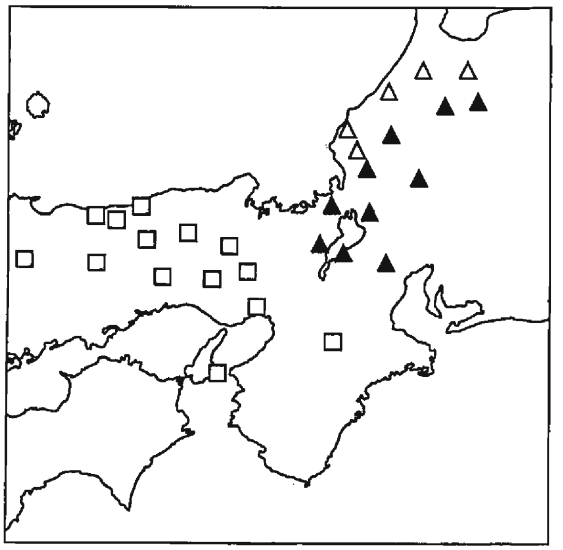

Fig. 12. Distribution of stations where later phase from event 14 was observed. Solid triangles show stations where later phase was observed. Open triangles show stations where later phase was not observed. Rectangles show stations which were not triggered by this event.

3. 6 Intermediate-depth earthquakes at Ryukyu islands

Triplication caused by the 410 km discontinuity is also observed in an event in the Ryukyu region. In event 7, the later phase was observed at an epicentral distance of 1050 km (**Fig. 13**). The apparent velocity of P and X phases is 8.5 km/s and 11.0 km/s, respectively. A later phase was observed at an epicentral distance between 1150 and 1250 km. The amplitude of the later phase is the same as that of the P phase at an epicentral distance of 1100 km and larger than that of direct P phase farther than 1150 km. From the epicentral distance and depth, we interpreted this later phase as a branch of triplication at 410 km discontinuity.

4. Discussion

In general, many later phases are observed on short period seismograms. However, the emergence of these phases is incoherent in some stations. Many later phases are observed at single stations only. This behavior shows that these phases are generated in the crust near the station. If the later phases were generated near the hypocenter, they would show coherency at each station. However, many of the observed later phases show scattering near the recording stations.

The observed amplitude of the later phases in this study is larger than that anticipated from the velocity contrasts of standard Earth models, which implies that large velocity contrast exists in the interface. In many cases, the estimated velocity contrast becomes too large. However, since a later phase is not observed in many events, actual velocity contrast in

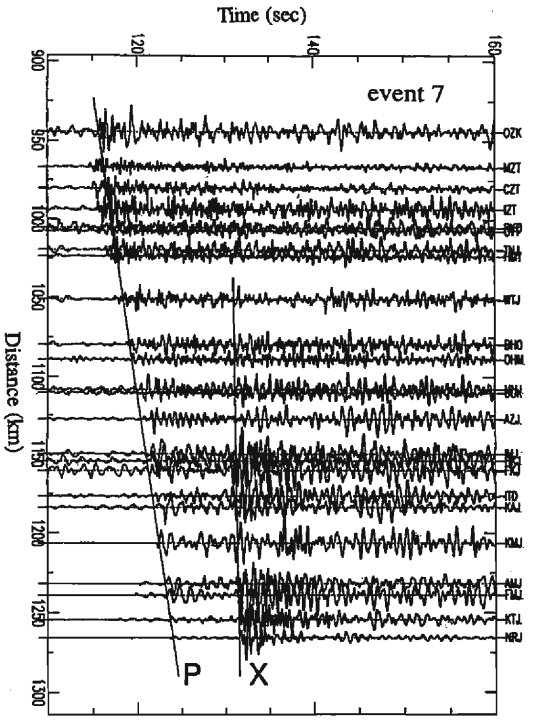

Fig. 13. Seismograms of event 7 which occurred at Ryukyu region. Time scale is reduced to t-D/11.0 (km/s). Initial and later arrivals are indicated by solid lines. Seismograms are filtered to pass the frequency bands of 0.5–2.0 Hz.

the boundary may be smaller than one estimated using the observed maximum amplitude of a later phase. Two models could possibly explain this discrepancy. The first model is where a large velocity contrast exists locally. To be feasible, however, this idea needs a large velocity contrast of as much as 10% in the mantle. Although the largest velocity discontinuity exists in the boundary between the slab and wedge mantle, the velocity contrast is still usually less than 7–8 % (Suyehiro and Sacks, 1979). An alternative idea is that the velocity contrast is small but the undulation of reflector generates an alternating focusing and defocusing effect. The second model appears to be more plausible to explain the locally observed X phase.

Moreover, analysis of multiple ScS reverberation shows that the shear wave impedance profiles imaged to 5.8% decrease roughly 330 km beneath the Japan Sea, Yellow Sea and eastmost Asia (Revenaugh and Jordan, 1991). As mentioned in section 3. 2, anomalous later phases are frequently observed in events occurring in the Japan Sea region. The upper mantle velocity in this region is clearly lower than that in other regions (Fukao et al., 1992). The observed later phases are possibly related to an anomalous structure in the upper mantle of eastmost Asia.

Further studies on both short period and broad band seismograms are required before a definitive answer to this question can be found.

5. Conclusions

Numerous phases are sometimes observed between P and S arrivals. From deep events in the Ryukyu and Hokkaido regions, branches of triplication are observed in our DPRI network. From deep events which occurred south of the Bonin region, we observed later phases whose apparent velocity is much smaller than that of the P phases. We infer the origin of these phases as being trapped phases in the crust near the Nankai trough. Moreover, a converted phase which is probably reflected or converted at the slab interface was also observed. Using these phases, we have shown that the hypocenters of deep earthquakes are located 20 km apart from an upper slab interface. In deep events below the Japan Sea region, anomalous later phases are likewise observed. These phases are possibly generated from a low velocity zone below the east Asia region.

Acknowledgements

We thank S. Sekiguchi for providing the 3D ray tracing and Gaussian-beam method program. We would also like to thank Takahiro Ohkura for his useful suggestions and discussions. We thank other members of our group for their valuable advice and encouragement in carrying out this work. Map and waveform plots were done using MAP (Sumisawa and Tapley, 1990) and SAC (Tull, 1988), respectively. We are also grateful to the staff of SWARMS for providing the seismic data.

References

Disaster Prevention Research Institute, Kyoto University (1986) : Seismic Wave Automatic Processing System at Disaster Prevention Research Institute, Kyoto University Report of the Coordinating Committee for Earthquake Prediction, Vol. 35, pp. 431–436 (in Japanese).

Fukao, Y., M. Obayashi, H. Inoue, and M. Nenbai (1992) : Subducting slabs stagnant in the mantle transition zone, J. Geophys. Res., Vol. 97, pp. 4809–4822.

Green, H. W. and P. C. Burnley (1989) : A new self-organizing mechanism for deep-focus earthquakes, Nature, Vol. 341, pp. 733–737.

Hasegawa, A., N. Umino and A. Takagi (1978) : Double-planed structure of the deep seismic zone in the northeastern Japan arc, Tectonophysics, Vol. 47, pp. 43–58.

Helfrich, G. R., S. Stein, and B. J. Wood (1989) : Subduction zone thermal structure and mineralogy and their relationship to seismic wave reflections and conversions at the slab/mantle interface, J. Geophys. Res., Vol. 94, pp. 753–763.

Hori, S., H. Inoue, Y. Fukao and M. Ukawa (1985) : Seismic detection of the untransformed 'basaltic' oceanic crust subducting into the mantle, Geophys. J. Roy. Astr. Soc., Vol. 83, pp. 169–197.

Iidaka, T. and M. Mizoue (1991) : P-wave velocity structure inside the subducting Pacific plate beneath the Japan region, Phys. Earth Planet. Inter., Vol. 66, pp. 203–213.

Ishida, M. (1984) : The spatial distribution of earthquake hypocenters and the three-dimensional velocity structure in the Kanto-Tokai District, Japan, J. Phys. Earth, Vol. 32, pp. 399–422.

Matsuzawa, T., N. Umino, A. Hasegawa, and A. Takagi (1986) : Upper mantle velocity structure estimated from PS-converted wave beneath the north-eastern Japan arc., Geophys. J. Roy. Astr. Soc., Vol. 86, pp. 767–787.

Matsuzawa, T., T. Kono, A. Hasegawa, and A. Takagi (1990) : Subducting plate boundary beneath the northeastern Japan arc estimated from SP converted waves. Tectonophysics, Vol. 181, pp. 123–133.

Obara, K. (1989) : Regional extent of the S wave reflector beneath the Kanto district, Japan, Geophys. Res. Lett., Vol. 16, pp. 839–842.

Ohkura, T., M. Ando and S. Kaneshima (1990) : Inhomogeneity of the discontinuity in a slab, Abstracts in the Seismological Society of Japan, No. 2, pp. 209 (in Japanese).

Park, C–H, K. Tamaki and K. Kobayashi (1990) : Age-depth correlation of the Philippine Sea back-arc basins and other marginal basins in the world, Tectonophysics, Vol. 181, pp. 351–371.

Revenaugh, J. and T. H. Jordan (1991) : Mantle layering from ScS reverberations 3. the upper mantle, J. Geophys. Res., Vol. 96, pp. 19781–19810.

Ringwood, A. E. and T. Irifune (1988) : Nature of the 650-km seismic discontinuity : implications for mantle dynamics and differentiation, Nature, Vol. 331, pp. 131–136

Sekiguchi, S. (1988) : A new seismic phase from earthquakes beneath the Japan Sea, generated near the Moho discontinuity, Res. Note of the National Res. Center for Disas. Prev., Vol. 78, pp. 1–12.

Senna, N., H. Oda and K. Seno (1990) : Regional Variation of Rayleigh wave group velocities in the Philippine Sea area, Zisin, Vol. 43, pp. 91–100, (in Japanese with English abstracts).

Sumisawa, K. E. and W. C. Tapley (1990) : MAP-A Cartographic Program For The Display of Seismic Data. Computer program available from Lawrence Livermore National Laboratory.

Suyehiro, K. and I. S. Sacks (1979) : P-and S-wave velocity anomalies associated with the subducting lithosphere determined from travel-time residuals in the Japan region, Bull. Seism. Soc. Amer., Vol. 69, pp. 97–114.

Tull, J. E. (1988) : SAC-Seismic analysis code. Computer program available from Lawrence Livermore National Laboratory.

Wu, T.–C., W. A. Basett, P. C. Burnley, and M. S. Weathers (1993) : Shear-promoted phase transitions in Fe2O4 and Mg2O4 and the mechanism of deep earthquakes, J. Geophys. Res., Vol. 98, pp. 19767–19776.